

KA-TP-4-1999
DESY 99-043
hep-ph/9903504

Precision Analysis of the Masses of the Neutral Higgs Bosons in the MSSM

S. HEINEMEYER^a, W. HOLLIK^{b,c} AND G. WEIGLEIN^c

^a *DESY Theorie, Notkestr. 85, 22603 Hamburg, Germany*

^b *Theoretical Physics Division, CERN, CH-1211 Geneva 23, Switzerland*

^c *Institut für Theoretische Physik, Universität Karlsruhe,
D-76128 Karlsruhe, Germany*

Abstract

The masses of the neutral \mathcal{CP} -even Higgs bosons in the Minimal Supersymmetric Standard Model (MSSM) are predicted on the basis of explicit Feynman-diagrammatic calculations. The results, containing the complete diagrammatic one-loop corrections, the leading two-loop corrections of $\mathcal{O}(\alpha\alpha_s)$ and further improvements taking into account leading electroweak two-loop and higher-order QCD contributions, are discussed and compared with results obtained by renormalization group calculations. Good agreement is found in the case of vanishing mixing in the scalar top sector, while sizable deviations occur if scalar top mixing is taken into account. By means of a Taylor expansion a compact approximation formula for the mass of the lightest Higgs boson, m_h , is derived. The quality of the approximation in comparison with the full result is analyzed.

PRECISION ANALYSIS OF THE MASSES OF THE NEUTRAL HIGGS BOSONS IN THE MSSM*

SVEN HEINEMEYER^a, WOLFGANG HOLLIK^{b,c} AND GEORG WEIGLEIN^c

^a DESY Theorie, Notkestr. 85, 22603 Hamburg, Germany

^b Theoretical Physics Division, CERN, CH-1211 Geneva 23, Switzerland

^c Institut für Theoretische Physik, Universität Karlsruhe,
D-76128 Karlsruhe, Germany

The masses of the neutral \mathcal{CP} -even Higgs bosons in the Minimal Supersymmetric Standard Model (MSSM) are predicted on the basis of explicit Feynman-diagrammatic calculations. The results, containing the complete diagrammatic one-loop corrections, the leading two-loop corrections of $\mathcal{O}(\alpha\alpha_s)$ and further improvements taking into account leading electroweak two-loop and higher-order QCD contributions, are discussed and compared with results obtained by renormalization group calculations. Good agreement is found in the case of vanishing mixing in the scalar top sector, while sizable deviations occur if scalar top mixing is taken into account. By means of a Taylor expansion a compact approximation formula for the mass of the lightest Higgs boson, m_h , is derived. The quality of the approximation in comparison with the full result is analyzed.

PACS numbers: 11.30.Pb, 12.38.Bx, 14.80.Cp

1. Introduction

The search for the lightest Higgs boson provides a direct and very stringent test of Supersymmetry (SUSY) and is one of the main goals at the present and the next generation of colliders. A precise prediction of its mass, m_h , is inevitable for determining the discovery and exclusion potential of LEP2 and the upgraded Tevatron in this search and for analyzing the accessible MSSM parameter space. If the MSSM Higgs boson exists, it will be detectable at the LHC and a future linear collider (LC), and its mass will be measured at these machines with high precision. The comparison of the MSSM prediction with the experimental value of m_h will then allow

* Talk given by G. Weiglein at the Cracow Epiphany Conference on Electron-Positron Colliders, Cracow, January 5–10, 1999.

a very sensitive test of the model. A precise knowledge of the mass of the heavier \mathcal{CP} -even Higgs boson, m_H , will be important for resolving the mass splitting between the \mathcal{CP} -even and -odd Higgs-boson masses.

The mass of the lightest Higgs boson in the MSSM is restricted at the tree level to be smaller than the Z -boson mass, M_Z . The dominant one-loop corrections arise from the top and scalar-top sector via terms of the form $G_\mu m_t^4 \ln(m_{\tilde{t}_1} m_{\tilde{t}_2} / m_t^2)$ [1]. These results have been improved by performing a complete one-loop calculation in the on-shell scheme [2–4]. Beyond one-loop order renormalization group (RG) methods have been applied in order to obtain leading logarithmic higher-order contributions [5–9]. Furthermore the leading two-loop QCD corrections have been calculated in the effective potential method [10, 11]. Phenomenological analyses for the neutral \mathcal{CP} -even Higgs-boson masses have until recently been based either on RG improved one-loop calculations [6, 7, 9] or on the complete Feynman-diagrammatic one-loop on-shell result [2–4]. The numerical results of these approaches however differ by up to 20 GeV in m_h .

Recently the Feynman-diagrammatic result for the dominant two-loop contributions of $\mathcal{O}(\alpha\alpha_s)$ to the masses of the neutral \mathcal{CP} -even Higgs bosons has become available [12]. By combining these contributions with the complete one-loop on-shell result [3], the currently most precise result for m_h based on diagrammatic calculations is obtained [13, 14]. It has been implemented into a Fortran program called *FeynHiggs* [15]. In the present paper the new Feynman-diagrammatic results are briefly summarized and compared with the results obtained by RG methods. Furthermore a compact analytical approximation formula [16] is discussed, which is derived from the full diagrammatic result by means of a Taylor expansion.

2. Diagrammatic two-loop calculation of the masses of the neutral \mathcal{CP} -even Higgs bosons

The MSSM Higgs sector can be described with the help of two parameters: $\tan\beta = v_2/v_1$, the ratio of the two vacuum expectation values, and M_A , the mass of the \mathcal{CP} -odd Higgs boson. The tree-level predictions for the masses m_h and m_H of the neutral \mathcal{CP} -even Higgs bosons h and H are determined by diagonalizing the tree-level mass matrix given in terms of the current eigenstates ϕ_1 and ϕ_2 . In the Feynman-diagrammatic approach the higher-order corrected Higgs-boson masses are derived by determining the poles of the h, H -propagator matrix whose inverse is given by

$$(\Delta_{\text{Higgs}})^{-1} = -i \begin{pmatrix} q^2 - m_{H,\text{tree}}^2 + \hat{\Sigma}_H(q^2) & \hat{\Sigma}_{hH}(q^2) \\ \hat{\Sigma}_{hH}(q^2) & q^2 - m_{h,\text{tree}}^2 + \hat{\Sigma}_h(q^2) \end{pmatrix}, \quad (1)$$

where the $\hat{\Sigma}$ denote the renormalized Higgs-boson self-energies, which can be decomposed according to

$$\hat{\Sigma}_s = \hat{\Sigma}_s^{(1)} + \hat{\Sigma}_s^{(2)} + \dots, \quad s = h, H, hH, \quad (2)$$

into the contributions at one-loop order, two-loop order etc.

For the one-loop contributions to these self-energies, $\hat{\Sigma}_s^{(1)}(q^2)$, we take the result of the complete one-loop on-shell calculation of Ref. [3]. The agreement with the result obtained in Ref. [2] is better than 1 GeV for almost the whole MSSM parameter space.

The leading two-loop corrections, $\hat{\Sigma}_s^{(2)}(0)$, have been obtained in Refs. [12–14] by calculating the $\mathcal{O}(\alpha\alpha_s)$ contribution of the t, \tilde{t} -sector to the renormalized Higgs-boson self-energies at zero external momentum from the Yukawa part of the theory. The calculation has been performed in the on-shell scheme. It involves a two-loop renormalization in the Higgs sector and a one-loop renormalization in the scalar top sector of the MSSM. The calculations have been performed using Dimensional Reduction (DRED) [17], which is necessary in order to preserve the relevant SUSY relations. In deriving these results, use has been made of the computer-algebra programs *FeynArts* [18] (in which the relevant part of the MSSM has been implemented) for generating the Feynman amplitudes, and *TwoCalc* [19] for evaluating the two-loop diagrams and counterterm contributions.

The results for the corrections in $\mathcal{O}(\alpha\alpha_s)$ are given in terms of the SUSY parameters $\tan\beta$, M_A , μ , $m_{\tilde{g}}$, $m_{\tilde{t}_1}$, $m_{\tilde{t}_2}$, and $\theta_{\tilde{t}}$, where μ denotes the Higgs-mixing parameter and $m_{\tilde{g}}$ the mass of the gluino. The mass eigenstates \tilde{t}_1, \tilde{t}_2 and the mixing angle $\theta_{\tilde{t}}$ in the scalar top sector are derived by diagonalizing the mass matrix of the scalar top quarks given in the basis of the current eigenstates \tilde{t}_L, \tilde{t}_R . The non-diagonal entry in the scalar quark mass matrix is proportional to the mass of the quark and reads for the \tilde{t} -mass matrix $m_t M_t^{LR} = m_t(A_t - \mu \cot\beta)$, where we have adopted the conventions as in Ref. [14]. Due to the large value of m_t these mixing effects are in general non-negligible.

Inserting the contributions in $\mathcal{O}(\alpha)$ and $\mathcal{O}(\alpha\alpha_s)$ into eq. (1) and determining the poles of the h, H -propagator matrix yields the prediction for the masses of the neutral \mathcal{CP} -even Higgs bosons. We have implemented two further corrections beyond $\mathcal{O}(\alpha\alpha_s)$ into the prediction for m_h : The first correction concerns leading QCD corrections beyond two-loop order, taken into account by using the $\overline{\text{MS}}$ top-quark mass

$$\overline{m}_t = \overline{m}_t(m_t) \approx m_t / \left(1 + \frac{4}{3\pi} \alpha_s(m_t) \right) \quad (3)$$

for the two-loop contributions instead of the pole mass m_t . The second one

is the leading two-loop Yukawa correction of $\mathcal{O}(G_\mu^2 m_t^6)$, taken over from the result obtained by RG methods [7, 20].

The results described above have been implemented into the Fortran program *FeynHiggs* [15], which needs about 0.5 seconds for the evaluation of m_h , m_H on a Sigma station (Alpha CPU, 600 MHz) for one set of parameters. As an additional constraint (besides the experimental bounds) on the squark masses, the program also evaluates the contribution to $\Delta\rho$ arising from \tilde{t}/\tilde{b} -loops up to $\mathcal{O}(\alpha\alpha_s)$ [21]. A value of $\Delta\rho$ outside the preferred region of $\Delta\rho^{\text{SUSY}} \lesssim 1 \cdot 10^{-3}$ [22] indicates experimentally disfavored \tilde{t} - and \tilde{b} -masses. The program *FeynHiggs* is available via the WWW page <http://www-itp.physik.uni-karlsruhe.de/feynhiggs>.

3. Numerical Results

For the numerical evaluation we have chosen two values for $\tan\beta$, which are favored by GUT scenarios [23]: $\tan\beta = 1.6$ for the SU(5) scenario and $\tan\beta = 40$ for the SO(10) scenario. Other parameters are $M_Z = 91.187$ GeV, $M_W = 80.39$ GeV, $G_\mu = 1.16639 \cdot 10^{-5}$ GeV $^{-2}$, $\alpha_s(m_t) = 0.1095$, and $m_t = 175$ GeV, if not otherwise indicated. Further parameters are M_A , $m_{\tilde{g}}$, μ , and the SU(2) soft SUSY-breaking parameter $M(\equiv M_2)$. The other gaugino mass parameter, M_1 , is fixed via the GUT relation $M_1 = (5 s_W^2)/(3 c_W^2) M$. In the figures below we have chosen $m_{\tilde{q}} \equiv M_{\tilde{t}_L} = M_{\tilde{t}_R}$ for the diagonal entries in the scalar top mass matrix.

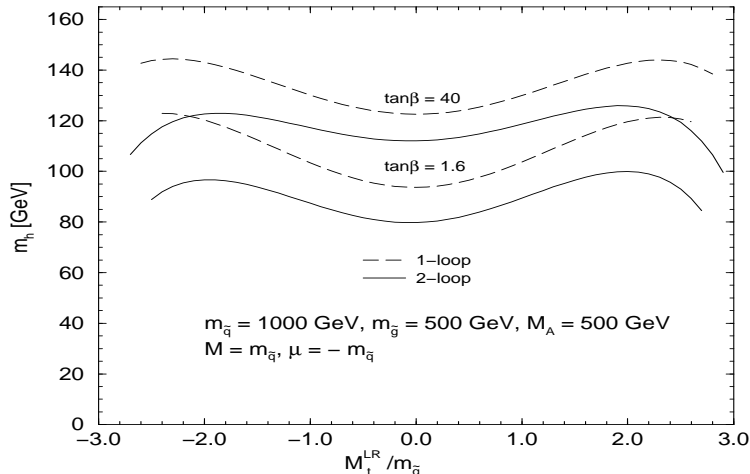


Fig. 1. One- and two-loop results for the mass of the lightest Higgs boson m_h as a function of $M_t^{LR}/m_{\tilde{q}}$ for two values of $\tan\beta$.

Fig. 1 shows the result for m_h obtained from the diagrammatic two-loop

calculation as a function of $M_t^{LR}/m_{\tilde{q}}$, where $m_{\tilde{q}}$ is fixed to 1000 GeV. The two-loop contributions give rise to a large reduction of the one-loop on-shell result by up to 20 GeV. A minimum in the prediction for m_h occurs around $M_t^{LR}/m_{\tilde{q}} = 0$, which corresponds to the case of no mixing in the \tilde{t} -sector. A maximum in the two-loop result for m_h is reached for about $|M_t^{LR}/m_{\tilde{q}}| \approx 2$, this case we refer to as ‘maximal mixing’. In the two-loop result the maxima are shifted compared to their one-loop values of about $|M_t^{LR}/m_{\tilde{q}}| \approx 2.4$. Varying $\tan\beta$ around the value $\tan\beta = 1.6$ leads to a relatively large effect in m_h , while the effect of varying $\tan\beta$ around $\tan\beta = 40$ is marginal. Different values of the gluino mass, $m_{\tilde{g}}$, in the two-loop contribution affect the prediction for m_h by up to ± 2 GeV in the maximal-mixing scenario, while the effect is negligible in the no-mixing scenario. Varying M , which enters via the non-leading one-loop contributions, changes the value of m_h by ± 1.5 GeV. A more detailed analysis of the dependence of our results on the different SUSY parameters has been performed in Ref. [14].

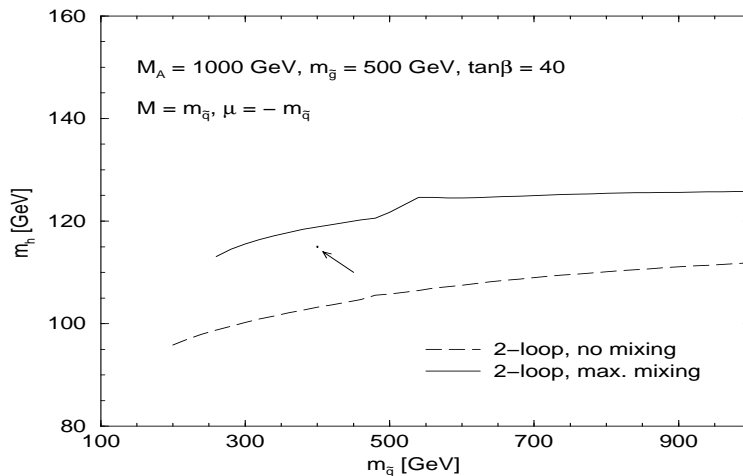


Fig. 2. The two-loop result for m_h as a function of $m_{\tilde{q}}$ in the no-mixing and the maximal-mixing case. The point marked by an arrow indicates the prospect for the experimental precision reached by a future linear collider in the determination of m_h and $m_{\tilde{q}}$ for the hypothetical values $m_h = 115$ GeV and $m_{\tilde{q}} = 400$ GeV.

If the lightest Higgs boson and Supersymmetric particles will be found at the next generation of colliders, the experimental value of m_h will be measured with high accuracy and also the possible range of the SUSY scale $m_{\tilde{q}}$ will in this case be constrained to a small interval. At a high-luminosity LC the prospect for the accuracy obtainable for these parameters is $\Delta m_h = 0.05$ GeV and $\Delta m_{\tilde{q}} = 0.1\%$. In Fig. 2 the two-loop result for m_h is shown as a function of $m_{\tilde{q}}$ in the no-mixing and the maximal-mixing case. The

parameter space in the $(m_h, m_{\tilde{q}})$ plane corresponding to the accuracy in m_h and $m_{\tilde{q}}$ at the LC is indicated in the plot for the hypothetical central values $m_h = 115$ GeV and $m_{\tilde{q}} = 400$ GeV. As can be seen from the plot, a precision determination of m_h and $m_{\tilde{q}}$ will provide a very sensitive consistency test of the model.

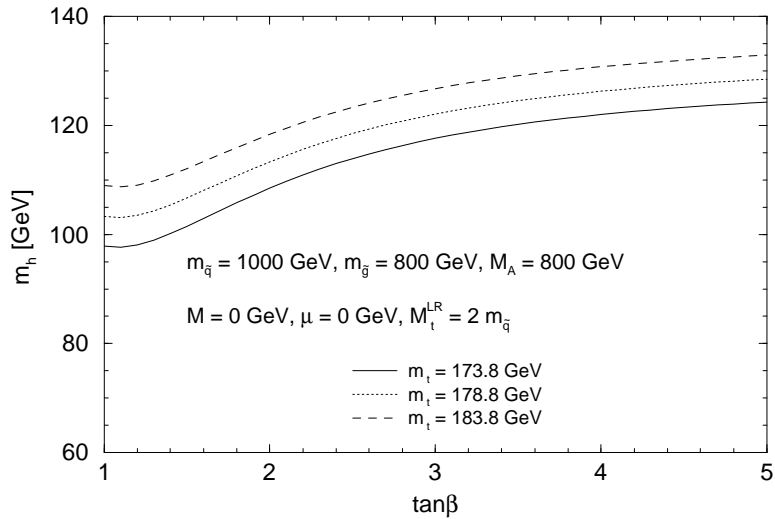


Fig. 3. The maximally possible value for m_h as a function of $\tan\beta$ for $m_{\tilde{q}} = 1000$ GeV and three different values of m_t .

In order to determine the maximally possible value for m_h within the MSSM as a function of $\tan\beta$, we have performed a parameter scan in which $m_{\tilde{g}}, M, \mu, M_A$ and M_t^{LR} have been varied for three values of m_t and fixed values of $m_{\tilde{q}}$ and $\tan\beta$. Fig. 3 shows the maximal Higgs-boson mass value in the range $\tan\beta \leq 5$ for $m_{\tilde{q}} = 1000$ GeV (in Fig. 3 the choice $M = \mu = 0$ has been made for simplicity; the change in m_h when these parameters are chosen at their experimental lower bounds is negligible). The upper bound is shown for the current experimental value of the top-quark mass, $m_t = 173.8$ GeV, and for values which are higher by one and two standard deviations, respectively. Our results confirm that for the scenario with $\tan\beta = 1.6$ practically the whole parameter space of the MSSM can be covered at LEP2. For slightly larger $\tan\beta$ and maximal mixing, however, some parameter space remains in which the Higgs boson could escape the detection at LEP2. For $\tan\beta = 40$, on the other hand, the prediction for m_h is at the edge of the LEP2 range even in the no-mixing case. The full exploration of the MSSM parameter space for the scenario with large $\tan\beta$ will be a challenge for the upgraded Tevatron, the LHC, and the LC.

4. Numerical comparison with the RG approach

We now turn to the comparison of our diagrammatic results with the predictions obtained via RG methods. The upper plot of Fig. 4 shows the prediction for m_h as a function of $M_t^{LR}/m_{\tilde{q}}$, corresponding to our diagrammatic result and to the result obtained by RG methods [8]. In the no-mixing case the diagrammatic result agrees well with the RG result. For non-vanishing \tilde{t} -mixing sizable deviations between the diagrammatic and the RG results occur, which can reach 5 GeV for moderate mixing and become very large for large values of $|M_t^{LR}/m_{\tilde{q}}|$. As already stressed above, the maximal value for m_h in the diagrammatic approach is reached for $|M_t^{LR}/m_{\tilde{q}}| \approx 2$, whereas the RG results have a maximum at $|M_t^{LR}/m_{\tilde{q}}| \approx 2.4$, i.e. at the one-loop value. Varying the value of $m_{\tilde{g}}$ in our result shifts the diagrammatic result relative to the RG result (which does not contain the gluino mass as a parameter) within ± 2 GeV in the region of large mixing.

In the upper plot of Fig. 4 the results of our diagrammatic on-shell calculation and the RG methods have been compared in terms of the parameters $M_{\tilde{t}_L}$, $M_{\tilde{t}_R}$ and M_t^{LR} of the \tilde{t} -mixing matrix. However, since the two approaches rely on different renormalization schemes, the meaning of these (non-observable) parameters is not precisely the same in the two approaches starting from two-loop order. In order to compare results obtained by different approaches making use of different renormalization schemes, we find it preferable to compare predictions for physical observables in terms of other observables (instead of unphysical parameters). As a step into this direction we compare in the lower plot of Fig. 4 the diagrammatic results and the RG results as a function of the physical mass $m_{\tilde{t}_2}$ and with the mass difference $\Delta m_{\tilde{t}} = m_{\tilde{t}_2} - m_{\tilde{t}_1}$ and the mixing angle $\theta_{\tilde{t}}$ as parameters. In the context of the RG approach the running \tilde{t} -masses, derived from the \tilde{t} -mass matrix, are considered as an approximation for the physical masses. As in the comparison performed above in terms of unphysical parameters, in the lower plot of Fig. 4 very good agreement is found between the results of the two approaches in the case of vanishing \tilde{t} -mixing. For the maximal mixing angle $\theta_{\tilde{t}} = -\pi/4$ (and $\Delta m_{\tilde{t}} = 340$ GeV, for which the maximal Higgs-boson masses are achieved), however, the diagrammatic result yields values for m_h which are higher by about 5 GeV.

The upper bound on m_h for a certain value of $\tan\beta$ derived from our diagrammatic results is thus higher in the low $\tan\beta$ region by about 5 GeV than the upper bound derived previously from the RG results. As a result, we find that the $\tan\beta$ region which can fully be covered at LEP2 and the upgraded Tevatron is significantly reduced compared to previous studies.

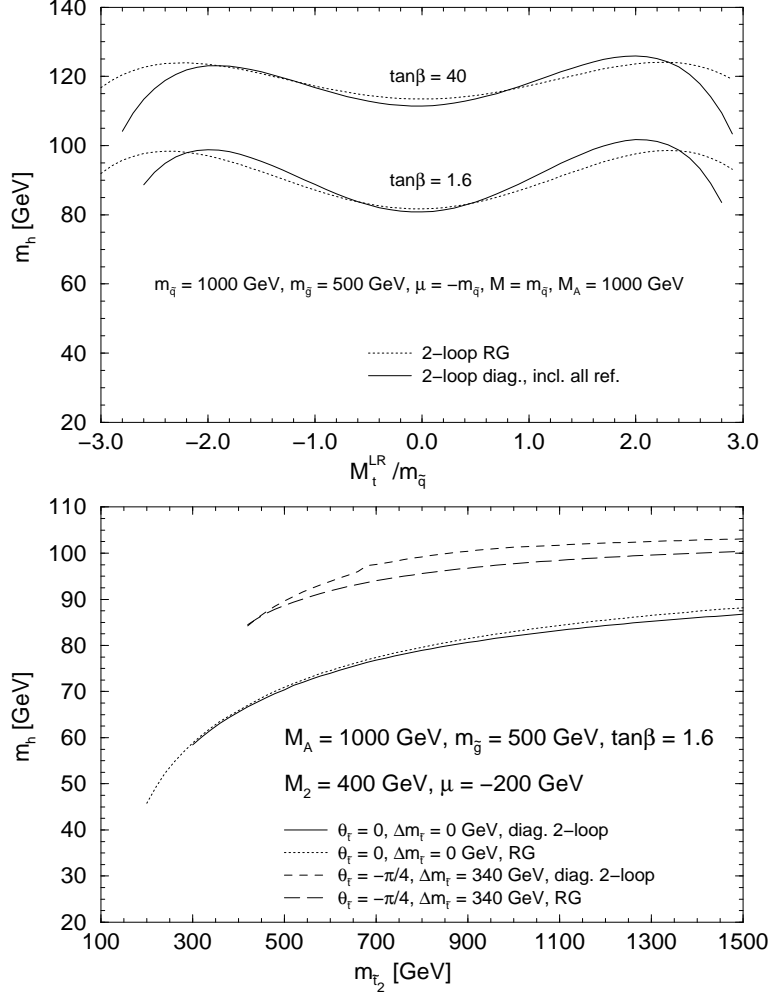


Fig. 4. Comparison between the Feynman-diagrammatic calculations and the results obtained by renormalization group methods [8]. In the upper plot the (unphysical) soft SUSY-breaking parameters of the \tilde{t} -mixing matrix are chosen as input, while in the lower plot the physical \tilde{t} -masses and the mixing angle $\theta_{\tilde{t}}$ are the input parameters. For the curves with $\theta_{\tilde{t}} = 0$ in the lower plot a mass difference $\Delta m_{\tilde{t}} = 0$ GeV is taken, whereas for $\theta_{\tilde{t}} = -\pi/4$ we choose $\Delta m_{\tilde{t}} = 340$ GeV, for which the maximal Higgs-boson masses are achieved.

5. Compact approximation formula for m_h

In order to extract the dominant contributions to m_h from the rather complicated full result, we have derived by means of a Taylor expansion

a short analytical approximation formula from the diagrammatic two-loop result [16]. It can easily be implemented into existing programs and allows a very fast numerical evaluation. Since the most important contributions have been isolated in this analytical formula, it is also helpful for a better qualitative understanding of the source of the dominant corrections.

In deriving the formula the following approximations have been made:

- The momentum dependence of the one-loop and two-loop self-energies $\hat{\Sigma}_s$, $s = h, H, hH$ has been neglected in eq. (1).
- The parameters M , $m_{\tilde{g}}$ have been chosen according to $M = m_{\tilde{g}} = \sqrt{M_S^2 - \overline{m}_t^2}$, where M_S is given by

$$M_S = \begin{cases} \sqrt{m_{\tilde{q}}^2 + \overline{m}_t^2} & : M_{\tilde{t}_L} = M_{\tilde{t}_R} = m_{\tilde{q}} \\ \left[M_{\tilde{t}_L}^2 M_{\tilde{t}_R}^2 + \overline{m}_t^2 (M_{\tilde{t}_L}^2 + M_{\tilde{t}_R}^2) + \overline{m}_t^4 \right]^{\frac{1}{4}} & : M_{\tilde{t}_L} \neq M_{\tilde{t}_R} \end{cases}$$

- Contributions from the t, \tilde{t} -sector up to the two-loop level:
The main step of our approximations consists of a Taylor expansion of the one-loop and two-loop contributions from the t, \tilde{t} -sector in the parameter

$$\Delta_{\tilde{t}} = \frac{|m_t M_t^{LR}|}{M_S^2} = \frac{m_{\tilde{t}_2}^2 - m_{\tilde{t}_1}^2}{m_{\tilde{t}_2}^2 + m_{\tilde{t}_1}^2}, \quad (4)$$

where terms proportional to M_Z^2 have been neglected in the \tilde{t} mass matrix. For the one-loop correction we have expanded up to $\mathcal{O}(\Delta_{\tilde{t}}^8)$. We have kept terms up to $\mathcal{O}(M_Z^4/m_t^4)$, while terms of $\mathcal{O}(M_Z^2/M_S^2)$ have been neglected. For the two-loop self-energies the expansion has been carried out up to $\mathcal{O}(\Delta_{\tilde{t}}^4)$. We have furthermore used the approximation $\mu = 0$ in the $\hat{\Sigma}_s(0)$. After extracting a common prefactor $(1/\sin^2 \beta)$ we have set otherwise $\sin \beta = 1$ in the non-logarithmic one-loop contributions, while the full dependence on $\sin \beta$ is kept in the logarithmic one-loop and the two-loop contributions. For a discussion of these approximations see Ref. [16].

- For the one-loop contributions from the other sectors of the MSSM the leading logarithmic approximation has been used [5].
- Corrections beyond $\mathcal{O}(\alpha\alpha_s)$:
Leading contributions beyond $\mathcal{O}(\alpha\alpha_s)$ have been taken into account by incorporating the leading two-loop Yukawa correction of $\mathcal{O}(G_\mu^2 m_t^6)$ [7, 20] and by expressing the t, \tilde{t} -contributions through the $\overline{\text{MS}}$ top-quark mass \overline{m}_t instead of the pole mass m_t according to eq. (3).

The approximation formula for m_h^2 is obtained by inserting the described approximations for the one-loop and two-loop self-energies $\hat{\Sigma}_s$ into the mass matrix eq. (1). The diagonalization of the mass matrix incorporates contributions to m_h^2 that are formally of higher order but are non-negligible in general. For large M_A these higher-order contributions are suppressed by inverse powers of M_A . Therefore it is possible for $M_A \gg M_Z$ to perform an expansion in the loop order, leading to a very compact formula for m_h^2 of the form

$$m_h^2 = m_h^{2,\text{tree}} + \Delta m_h^{2,\alpha,t/\tilde{t}} + \Delta m_h^{2,\alpha,\text{rest}} + \Delta m_h^{2,\alpha\alpha_s} + \Delta m_h^{2,\alpha^2}. \quad (5)$$

The tree-level prediction and the one-loop contribution from the t, \tilde{t} -sector are given by

$$\begin{aligned} m_h^{2,\text{tree}} &= \frac{1}{2} \left[M_A^2 + M_Z^2 - \sqrt{(M_A^2 + M_Z^2)^2 - 4M_Z^2 M_A^2 \cos^2 2\beta} \right], \quad (6) \\ \Delta m_h^{2,\alpha,t/\tilde{t}} &= \frac{G_\mu \sqrt{2}}{\pi^2} \bar{m}_t^4 \left[\log \left(\frac{\bar{m}_t^2}{M_S^2} \right) \left\{ -\frac{3}{2} - \frac{3}{4} \frac{M_Z^2}{\bar{m}_t^2} \cos 2\beta - \frac{M_Z^4}{\bar{m}_t^4} \Lambda \cos^2 2\beta \right. \right. \\ &\quad \left. \left. - \frac{M_Z^2}{M_A^2} \cos^2 \beta \cos 2\beta \left(6 + \frac{3}{2} \frac{M_Z^2}{\bar{m}_t^2} (1 - 4 \sin^2 \beta) - \frac{M_Z^4}{\bar{m}_t^4} 8\Lambda \cos 2\beta \sin^2 \beta \right) \right\} \right. \\ &\quad \left. + \left\{ \frac{1}{4} \frac{M_Z^2}{\bar{m}_t^2} - \frac{11}{80} \frac{M_Z^4}{\bar{m}_t^4} + \frac{(M_t^{LR})^2}{M_S^2} \left(\frac{3}{2} - \frac{1}{2} \frac{M_Z^2}{\bar{m}_t^2} - \frac{3}{4} \frac{\bar{m}_t^2}{M_S^2} \right) \right. \right. \\ &\quad \left. \left. + \frac{(M_t^{LR})^4}{M_S^4} \left(-\frac{1}{8} + \frac{1}{2} \frac{\bar{m}_t^2}{M_S^2} - \frac{3}{8} \frac{\bar{m}_t^4}{M_S^4} \right) \right. \right. \\ &\quad \left. \left. + \frac{(M_t^{LR})^6}{M_S^6} \left(-\frac{3}{40} \frac{\bar{m}_t^2}{M_S^2} + \frac{3}{10} \frac{\bar{m}_t^4}{M_S^4} - \frac{1}{4} \frac{\bar{m}_t^6}{M_S^6} \right) \right. \right. \\ &\quad \left. \left. + \frac{(M_t^{LR})^8}{M_S^8} \left(-\frac{3}{56} \frac{\bar{m}_t^4}{M_S^4} + \frac{3}{14} \frac{\bar{m}_t^6}{M_S^6} - \frac{3}{16} \frac{\bar{m}_t^8}{M_S^8} \right) \right\} \times \right. \\ &\quad \left. \left(1 + 4 \frac{M_Z^2}{M_A^2} \cos^2 \beta \cos 2\beta \right) \right], \quad (7) \end{aligned}$$

where $\Lambda = \left(\frac{1}{8} - \frac{1}{3} s_w^2 + \frac{4}{9} s_w^4 \right)$, $s_w^2 = 1 - \frac{M_W^2}{M_Z^2}$.

The dominant two-loop contribution of $\mathcal{O}(\alpha\alpha_s)$ to m_h^2 reads:

$$\Delta m_h^{2,\alpha\alpha_s} = -\frac{G_\mu \sqrt{2}}{\pi^2} \frac{\alpha_s}{\pi} \bar{m}_t^4 \left[4 + 3 \log^2 \left(\frac{\bar{m}_t^2}{M_S^2} \right) + 2 \log \left(\frac{\bar{m}_t^2}{M_S^2} \right) - 6 \frac{M_t^{LR}}{M_S} \right]$$

$$\begin{aligned}
& - \frac{(M_t^{LR})^2}{M_S^2} \left\{ 3 \log \left(\frac{\overline{m}_t^2}{M_S^2} \right) + 8 \right\} \\
& + \frac{17 (M_t^{LR})^4}{12 M_S^4} \left] \left(1 + 4 \frac{M_Z^2}{M_A^2} \cos^2 \beta \cos 2\beta \right). \quad (8)
\end{aligned}$$

For the one-loop contribution from the other sectors of the MSSM, $\Delta m_h^{2,\alpha,\text{rest}}$, and the leading two-loop Yukawa correction, $\Delta m_h^{2,\alpha^2}$, which are numerically less important than the contributions given above, we refer to Ref. [16]. In the contributions from the t, \tilde{t} -sector at one-loop and two-loop order, eqs. (7) and (8), we have included correction factors of $\mathcal{O}(M_Z^2/M_A^2)$. In this way the compact formula (5) gives a reliable approximation for M_A values down to at least $M_A = 200$ GeV. The approximation formula for the general case of M_A is given in Ref. [16].

The contribution of $\mathcal{O}(\alpha\alpha_s)$ given in eq. (8) can be compared with analytical formulas derived via the two-loop effective potential approach for the case of no mixing in the \tilde{t} sector [10] and via RG methods [7,9]. The leading term $\sim \log^2(\overline{m}_t^2/M_S^2)$ agrees with the results in Refs. [7,9,10]. The subleading term for vanishing \tilde{t} -mixing $\sim \log(\overline{m}_t^2/M_S^2)$ agrees with the result of the two-loop effective potential approach [10] and the result of the two-loop RG calculation [9,10], but differs from the RG improved one-loop result [7,9]. The term $\sim \log(\overline{m}_t^2/M_S^2)(M_t^{LR}/M_S)^2$ for non-vanishing \tilde{t} -mixing differs from the result given in Ref. [7,9]. All other terms of $\mathcal{O}(\alpha\alpha_s)$ are new. The term $\sim M_t^{LR}/M_S$ shows that the result for m_h is not symmetric in $\pm M_t^{LR}$. The good numerical agreement with the RG results in the case of no mixing in the \tilde{t} sector can qualitatively be understood by noting that in the no-mixing case the leading term in both approaches agrees, while for the corrections proportional to powers of M_t^{LR}/M_S deviations occur already in the leading contribution.

The compact approximation formula has been implemented into *FeynHiggs*, in order to allow a direct comparison between the full result and the approximation, and is also provided as a separate program called *FeynHiggsFast*. The improvement in the speed of the evaluation with *FeynHiggsFast* compared to *FeynHiggs* is about a factor of 3×10^4 . In Fig. 5 the approximation formula is compared with the full result (in the lower plot the formula for general M_A is applied). The compact formula approximates the full result better than about 2 GeV for most parts of the MSSM parameter space. Larger deviations can occur for $|M_t^{LR}/m_{\tilde{q}}| > 2$.

G.W. thanks M. Jeżabek and the other organizers of the Epiphany Conference for the invitation, the excellent organization and the pleasant atmosphere during the Conference.

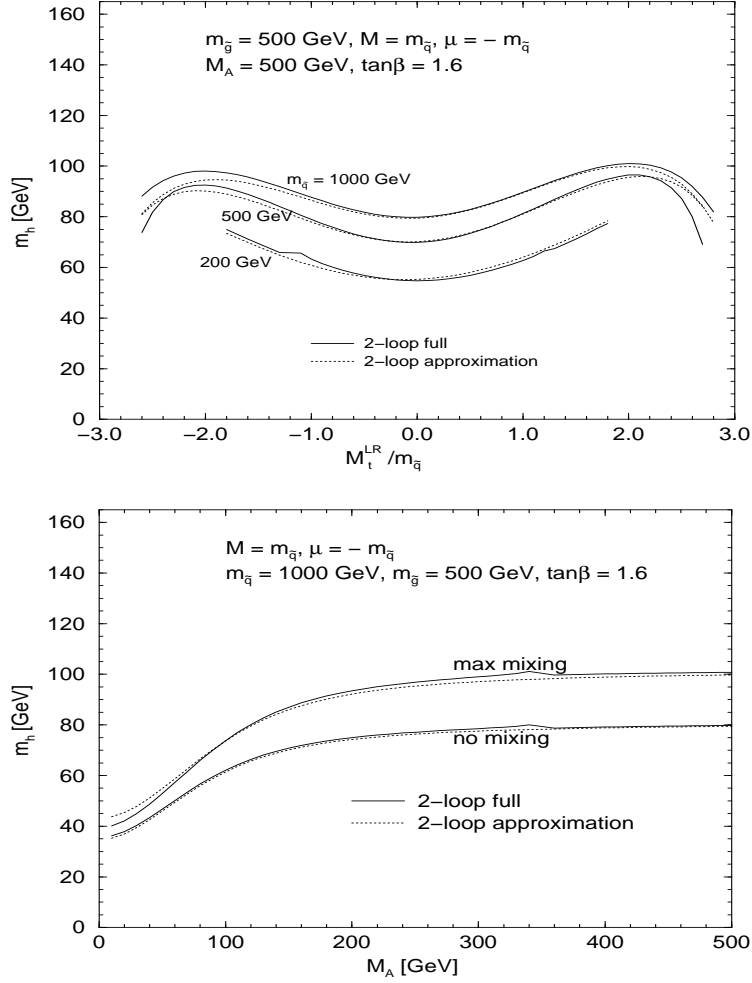


Fig. 5. Comparison between the approximation formula and the full diagrammatic result for m_h .

REFERENCES

- [1] H. Haber and R. Hempfling, *Phys. Rev. Lett.* **66** (1991) 1815;
Y. Okada, M. Yamaguchi and T. Yanagida, *Prog. Theor. Phys.* **85** (1991) 1;
J. Ellis, G. Ridolfi and F. Zwirner, *Phys. Lett. B* **257** (1991) 83; *Phys. Lett. B* **262** (1991) 477;
R. Barbieri and M. Frigeni, *Phys. Lett. B* **258** (1991) 395.
- [2] P. Chankowski, S. Pokorski and J. Rosiek, *Nucl. Phys. B* **423** (1994) 437.
- [3] A. Dabelstein, *Nucl. Phys. B* **456** (1995) 25; *Z. Phys. C* **67** (1995) 495.
- [4] J. Bagger, K. Matchev, D. Pierce and R. Zhang, *Nucl. Phys. B* **491** (1997) 3.

- [5] H. Haber and R. Hempfling, *Phys. Rev. D* **48** (1993) 4280.
- [6] J. Casas, J. Espinosa, M. Quirós and A. Riotto, *Nucl. Phys. B* **436** (1995) 3, E: *ibid.* **B 439** (1995) 466.
- [7] M. Carena, J. Espinosa, M. Quirós and C. Wagner, *Phys. Lett. B* **355** (1995) 209.
- [8] M. Carena, M. Quirós and C. Wagner, *Nucl. Phys. B* **461** (1996) 407.
- [9] H. Haber, R. Hempfling and A. Hoang, *Z. Phys. C* **75** (1997) 539.
- [10] R. Hempfling and A. Hoang, *Phys. Lett. B* **331** (1994) 99.
- [11] R.-J. Zhang, *Phys. Lett. B* **447** (1999) 89.
- [12] S. Heinemeyer, W. Hollik and G. Weiglein, *Phys. Rev. D* **58** (1998) 091701.
- [13] S. Heinemeyer, W. Hollik and G. Weiglein, *Phys. Lett. B* **440** (1998) 296.
- [14] S. Heinemeyer, W. Hollik and G. Weiglein, CERN-TH/98-405, hep-ph/9812472, to appear in *Eur. Phys. Jour. C*.
- [15] S. Heinemeyer, W. Hollik and G. Weiglein, CERN-TH/98-389, hep-ph/9812320.
- [16] S. Heinemeyer, W. Hollik and G. Weiglein, CERN-TH/99-74, hep-ph/9903404.
- [17] W. Siegel, *Phys. Lett. B* **84** (1979) 193;
D. Capper, D. Jones and P. van Nieuwenhuizen, *Nucl. Phys. B* **167** (1980) 479.
- [18] J. Küblbeck, M. Böhm and A. Denner, *Comp. Phys. Commun.* **60** (1990) 165.
- [19] G. Weiglein, R. Scharf and M. Böhm, *Nucl. Phys. B* **416** (1994) 606.
- [20] M. Carena, P. Chankowski, S. Pokorski and C. Wagner, *Phys. Lett. B* **441** (1998) 205.
- [21] A. Djouadi, P. Gambino, S. Heinemeyer, W. Hollik, C. Jünger and G. Weiglein, *Phys. Rev. Lett.* **78** (1997) 3626; *Phys. Rev. D* **57** (1998) 4179.
- [22] G. Altarelli, hep-ph/9811456.
- [23] M. Carena, S. Pokorski and C. Wagner, *Nucl. Phys. B* **406** (1993) 59;
W. de Boer et al., *Z. Phys. C* **71** (1996) 415.